Quantum Vortices Leave a Macroscopic Signature in the Thermal Background

Luca Galantucci,[1,2,*] Giorgio Krstulovic,[3,†] and Carlo F. Barenghi[2,‡]
[1]Istituto per le Applicazioni del Calcolo M. Picone, IAC-CNR, Via dei Taurini 19, Roma 00185, Italy
[2]School of Mathematics, Statistics and Physics, Newcastle University, Newcastle upon Tyne NE1 7RU, United Kingdom
[3]Université Côte d'Azur, Observatoire de la Côte d'Azur, CNRS, Laboratoire J. L. Lagrange, Boulevard de l'Observatoire CS 34229–F 06304 NICE Cedex 4, France

(Received 19 January 2025; revised 2 October 2025; accepted 22 October 2025; published 2 January 2026)

Recent work has highlighted the remarkable properties of quantum turbulence in superfluid helium II, consisting of a disordered tangle of quantized vortex lines which interact with each other and reconnect when they collide. According to Landau's two-fluid theory, these vortex lines move in a surrounding of thermal excitations called the *normal fluid*. Until now, the normal fluid has often been considered a passive background which simply provides the vortex lines with a mechanism for dissipating their kinetic energy into heat. Using a model which fully takes into account the two-way interaction between the vortex lines and the normal fluid, here we show numerically that each vortex line creates a macroscopic wake in the normal fluid that can be larger than the average distance between vortex lines; this is surprising, given the microscopic size of the superfluid vortex cores which induce these wakes. We show that in heat transfer experiments, the flow of the normal fluid can therefore be described as the superposition of an imposed uniform flow and wakes generated by the vortex lines, leading to nonclassical statistics of the normal fluid velocity. We also argue that this first evidence of independent fluid structures in the thermal excitations postulated by Landau may be at the root of recent, unaccounted for, experimental findings.

DOI: 10.1103/xnyc-321m

It was Landau who first understood that the properties of a many-body quantum system such as helium II depend on thermally excited elementary excitations—collective modes which he called phonons and rotons depending on whether their dispersion relation is linear or quadratic. This idea has influenced many areas of modern physics since. In the context of liquid helium, Landau's intuition led to the formulation of the two-fluid theory, which accounts for unusual behaviors of helium II, from second sound and thermal counterflows [1] to critical velocities [2]. Briefly, helium II behaves as the mixture of two inseparable fluid components: the viscous normal fluid (associated with the thermal excitations) and the inviscid superfluid (associated with the ground state). Each component has its own density field and velocity field, ρ_s, $\mathbf{v}_s$ for the superfluid and ρ_n, $\mathbf{v}_n$ for the normal fluid, where $\rho = \rho_n + \rho_s$ is the total density. As a consequence, two distinct motions occur simultaneously at the same position in space. Of the two components, only the normal fluid has nonzero entropy (hence, is capable of carrying heat). Because of quantum mechanical constraints, the superfluid's vorticity is concentrated to vortex lines of quantized circulation (in units of h/m where h is Planck's constant and m is the mass of one helium atom) and microscopic thickness (the vortex core radius is only $a_0 \approx 0.1$ nm). Over the years, the vortex lines have attracted great attention, revealing remarkable properties: vortex lattices [3], vortex nucleation [4], Kelvin waves [5,6], vortex reconnections [7], and quantum turbulence [8] of various kinds [9].

In contrast, much less attention has been paid to the normal fluid, of which we still know very little. We know that Landau's excitations are scattered by the velocity field of the vortex lines, creating a mutual friction between the two fluid components which allows energy exchange [10,11]. For the sake of simplicity, in most problems it is usually assumed that the normal fluid is spatially uniform or at rest, simply providing a dissipative background to the vortex lines.

Based on the mean free path λ and the Knudsen number λ/d, the description of Landau's excitations as a fluid (rather than a ballistic gas) is appropriate for length scales $d > 0.2$ μm at $T = 1.5$ K and $d > 0.02$ μm at $T = 2.1$ K, which is the temperature range of interest here. These values of d are safely smaller than both the size of tracer particles used to visualize flows ($\gtrsim 1$ μm) [12–16] and the typical distance between vortex lines in turbulence

*Contact author: luca.galantucci@cnr.it
†Contact author: giorgio.krstulovic@oca.eu
‡Contact author: carlo.barenghi@newcastle.ac.uk

experiments, $\ell \approx 10$ to 100 μm. It is therefore natural to assume that the normal fluid obeys no-slip boundary conditions, but what should be the normal fluid's large-scale velocity profile in a channel is still an open question. For coflows ($\mathbf{v}_s$ and $\mathbf{v}_n$ flowing in the same direction, e.g., driven by bellows) a laminar normal fluid profile has been observed [17] but its scaling with the Reynolds number has not been explained yet. For counterflows ($\mathbf{v}_s$ and $\mathbf{v}_n$ flowing in the opposite direction driven by a heater) there is theoretical debate about the shape of the laminar profile [18,19], and experimental evidence (but no quantitative information) of a transition to turbulence at large velocity [20,21]. Until now, no other flow structure, at any scale, has ever been identified in the normal fluid, which has remained somewhat mysterious.

The numerical results that we present here predict that the relative motion of vortex lines and the normal fluid creates, besides small dipolar structures [22] which are probably too small to be observed, also large macroscopic wakes in the normal fluid. The wakes are so large (even larger than the typical intervortex distance ℓ) that we infer from our data that they affect the velocity statistics of the normal fluid, producing skewed distributions with wide tails, strikingly dissimilar from classical turbulence. We shall see that some indirect evidence of this effect has been measured in counterflow turbulence experiments without being recognized.

Our numerical simulations of counterflow turbulence use the model FOUCAULT [23]. The code models vortex lines as space curves of infinitesimal thickness, which is appropriate given the huge separation of scales between the vortex core thickness a_0 and the typical distance ℓ between vortex lines in quantum turbulent flows. Unlike the original one-way approach of Schwarz [24], FOUCAULT accounts for the two-way interaction between the vortex lines (which evolve according to the Biot-Savart law and mutual friction corrections) and the normal fluid (which evolves according to a modified Navier-Stokes equation) [25]; as in the approach of Schwarz, vortex reconnections are implemented algorithmically. For simplicity our calculations are performed in a cube of size $D = 0.1$ cm with periodic boundary conditions (see Methods for details).

To model thermal counterflow, we impose average normal fluid and superfluid velocities along the positive and negative z directions, respectively. This creates a counterflow velocity $v_{ns} = |\bar{v}_n^z - \bar{v}_s^z|$ (where overbars denote spatial averages) which, in the experiments, is proportional to the applied heat flux. The two fluid components flow in opposite directions: the normal fluid carries the heat away from the heater at speed $\bar{v}_n^z = (\rho_s/\rho)v_{ns}$, while the superfluid flows in the opposite direction to conserve mass, $\bar{v}_s^z = -(\rho_n/\rho)v_{ns}$. The initial condition consists of few random vortex rings, which, after a transient, evolve into a statistically steady state, which is independent of the initial condition; at this point the vortex line density (defined as the length of vortex lines per unit volume) fluctuates around a mean value L corresponding to the average intervortex distance $\ell \approx 1/\sqrt{L}$. Our numerical experiments are performed at temperature $T = 1.5$ K at two distinct values of the counterflow velocity: $v_{ns}^{(1)} = 0.27$ cm/s and $v_{ns}^{(2)} = 0.94$ cm/s, yielding $L^{(1)} = 7.2 \times 10^2$ cm^{-2} and $L^{(2)} = 1.1 \times 10^4$ cm^{-2}, respectively. These turbulent vortex tangles are anisotropic, as vortices tend to lie on xy planes perpendicular to the applied counterflow in the z direction.

Figure 1 shows snapshots of the computed vortex tangles corresponding to $v_{ns} = v_{ns}^{(1)}$ (left) and $v_{ns} = v_{ns}^{(2)}$ (right). The superfluid vortices are displayed as green curves, and the enstrophy of the normal fluid, defined as $\Omega(\mathbf{x}) = |\boldsymbol{\omega}_n(\mathbf{x})|^2/2$ (where $\boldsymbol{\omega}_n = \nabla \times \mathbf{v}_n$) and normalized by its maximum value $\Omega_{\max}$, is rendered in reddish colors according to the color map reported on the left. At the bottom of each panel, we report a two-dimensional slice on a plane at fixed $y = y_0$ of the relative magnitude of in-plane normal fluid fluctuations $\Delta v_n(x,z) = \|\delta\tilde{\mathbf{v}}_n(x,y_0,z)\|/|\bar{v}_n^z|$, with $\delta\tilde{\mathbf{v}}_n = (v_n^x, v_n^z - \bar{v}_n^z)$, color coded by the color map on the right.

Previous calculations [22,26,27] have shown that each superfluid vortex is surrounded by two localized regions of large normal fluid enstrophy, essentially a vorticity dipole induced by the friction. This dipole is small, of the order of only a few micrometers (≈2 to 4 μm [26]). The novel effect which here we report is the existence of much larger normal fluid structures, whose existence has been to some extent speculated [28], but not clearly observed. The two-dimensional slices for both low (left) and high (right) counterflow velocity regimes reported in Fig. 1, clearly show that in the proximity of superfluid vortices there are regions (almost 2 orders of magnitude larger than the dipoles) where $\mathbf{v}_n$ is significantly different from $\bar{\mathbf{v}}_n$ (the magnitude of the normal fluid velocity fluctuations being up to 10% the applied normal fluid velocity $\bar{v}_n^z$). This is the first clear evidence of large scale (potentially observable experimentally) fluid structures which spontaneously appear in Landau's sea of thermal excitations.

Such large scale structures strongly modify and impact the statistical distribution of the normal fluid velocity. We concentrate the attention on the streamwise and spanwise velocity fluctuations, defined as $\delta v_n^z = v_n^z - \bar{v}_n^z$ and $\delta v_n^x = v_n^x$ (since $\bar{v}_n^x = 0$), respectively. In Fig. 2 we plot the probability distribution functions (PDFs) of the velocity fluctuations normalized by their respective variances σ_z and σ_x, for both counterflow values. $v_{ns}^{(1)} = 0.27$ cm/s (red) and $v_{ns}^{(2)} = 0.94$ cm/s (green), where σ_z and σ_x are the standard deviations of streamwise and spanwise velocities, respectively.

The main result, shown in the left panel of Fig. 2, is that the PDFs of the streamwise velocity fluctuations are left skewed, showing the predominance of negative

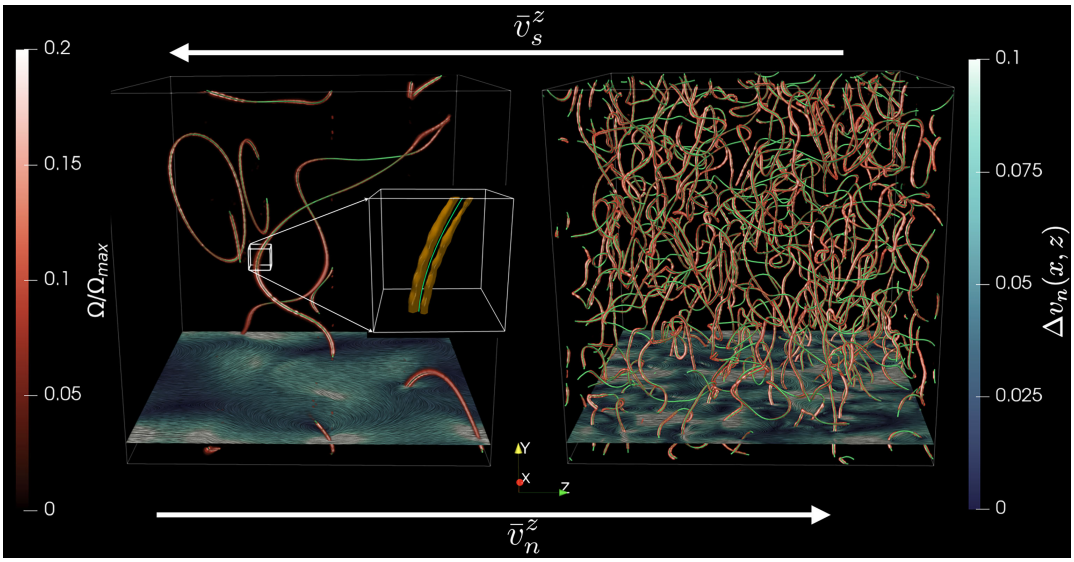

FIG. 1. Snapshots of vortex tangles. Turbulence at $T = 1.5$ K generated by counterflow velocities $v_{ns}^{(1)} = 0.27$ cm/s (left) and $v_{ns}^{(2)} = 0.94$ cm/s (right). The superfluid vortex lines are displayed as green curves and the normal fluid dipoles are visualized by the normalized enstrophy $\Omega(\mathbf{x})/\Omega_{\max}$ in reddish color. The relative magnitude of normal fluid fluctuations $\Delta v_n(x,z)$ is plotted on a xz plane at constant y.

fluctuations. In other words there are large regions where the normal fluid flows slower than the average flow in the direction parallel to the applied counterflow. In the spanwise direction, on the contrary, the PDFs are symmetrical—see the right panel of Fig. 2. This effect is independent of the counterflow velocity; in the low counterflow case (red curves), we observe that the tails have an exponential behavior.

Additionally, we find that, consistently with particle tracking velocimetry (PTV) experiments at not too small counterflow velocities [29], the standard deviation of the streamwise velocity is larger than its spanwise counterpart: $\sigma_z \approx 2\sigma_x$, as clearly shown in the insets of Fig. 2. As we move from the low to high velocity regime, the tails and the skewness of the PDFs become less pronounced, while the standard deviations increase ($\sigma/v_{ns} \sim$ constant, Fig. 2 insets), again as observed experimentally [29]. Furthermore, the normalized standard deviation slightly increases with temperature. We conclude that the PDFs of the normal fluid in counterflow turbulence differ strikingly from the PDFs of velocity fluctuations in classical turbulence, which display a sub-Gaussian behavior [30].

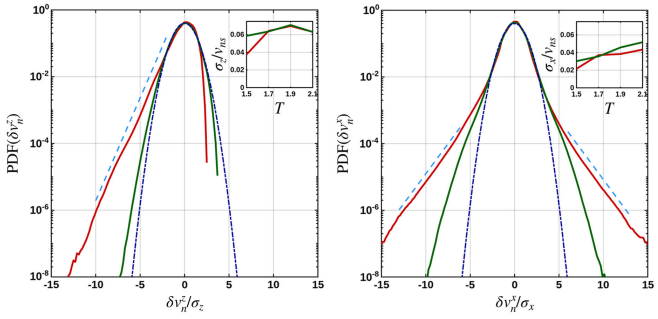

FIG. 2. PDFs of velocity fluctuations. Calculations at $T = 1.5$ K at the same parameters as Fig. 1. Left: streamwise PDF(δv_n^z) vs $\delta v_n^z/\sigma_z$ where σ_z is the standard deviation. Right: spanwise PDF(δv_n^x) vs $\delta v_n^x/\sigma_x$ where σ_x is the standard deviation. Red curves refer to $v_{ns}^{(1)} = 0.27$ cm/s and green curves to $v_{ns}^{(2)} = 0.94$ cm/s. Gaussian distributions are showed in the dot-dashed dark blue line for reference. Dashed cyan curves are exponential fits to the wide tails. Insets. Left (right): streamwise (spanwise) normalized standard deviation σ_z/v_{ns} (σ_x/v_{ns}) as a function of temperature T. Colors as in main figure.

We argue that the low-velocity regions—the regions which we have identified in Fig. 1—are wakes generated by the mutual friction force exerted by the vortex lines on the normal fluid. In fact, we find that the average speed of the vortex lines is about one tenth of $\bar{v}_n^z$ for both $v_{ns}^{(1)}$ and $v_{ns}^{(2)}$. Essentially, vortices are like obstacles which modify the normal fluid velocity [11,31], slowing down the normal fluid in the downstream region. As v_{ns} increases, the impact of these wakes on the PDFs is less pronounced (the PDFs tend to have a more Gaussian character) because wakes overlap, randomizing the flow.

In order to support our argument, we perform a numerical experiment in a simpler set-up, which clarifies the physics: a single, straight superfluid vortex oriented in the positive y direction in the presence of counterflow in the z direction, at the same values of T and v_{ns} used for Fig. 1. We find that, after a short transient, the vortex moves at constant relative velocity with respect to the normal fluid. In a turbulent tangle, vortices move at a relatively constant velocity with respect to the normal fluid only for a fraction

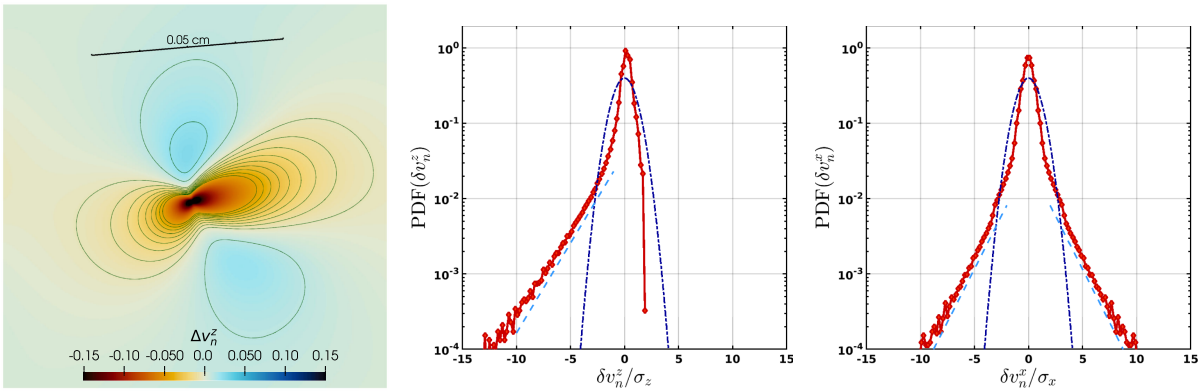

FIG. 3. Single vortex wake. Temperature $T = 1.5$ K and $v_{ns}^{(1)} = 0.27$ cm/s. Left column: relative normal fluid streamwise velocity fluctuations $\Delta v_n^z = \delta v_n^z/\bar{v}_n^z = (v_n^z(x,z) - \bar{v}_n^z)/\bar{v}_n^z$ vs x and z at fixed y_0. The ruler indicates the direction of the relative velocity of the single vortex line with respect to the normal fluid. Center column: PDF(δv_n^z) vs $\delta v_n^z/\sigma_z$, where $\delta v_n^z = v_n^z - \bar{v}_n^z$ and σ_z is the standard deviation. Right column: PDF(δv_n^x) vs $\delta v_n^x/\sigma_x$, where $\delta v_n^x = v_n^x$ ($\bar{v}_n^x = 0$) and σ_x is the standard deviation. Gaussian distributions are showed in dot-dashed dark blue line for reference. The dashed cyan lines are exponential functions to guide the eye.

of the time between two successive reconnections τ_r, which can be estimated using the vortex line density L as $\tau_r \approx 6\pi/|\kappa L \ln(L^{1/2}a_0)|$ [32]. Consequently, we consider the pattern of the normal fluid past the single vortex at time $t \approx \tau_r/10$. Figure 3 displays the results of this numerical experiment using the counterflow velocity $v_{ns}^{(1)}$ (equivalent figures for $v_{ns}^{(2)}$ are provided in Supplemental Material [33]).

The left panel of Fig. 3, where contour lines are drawn at constant values of $[v_n^z(x,z) - \bar{v}_n^z]/\bar{v}_n^z$, shows that the normal fluid wake is almost parabolic. The size of the wake, computed as a velocity weighed distance from the vortex [33], is $w^{(1)} = 190$ μm for $v_{ns} = v_{ns}^{(1)}$ and $w^{(2)} = 140$ μm for $v_{ns} = v_{ns}^{(2)}$, almost 2 orders of magnitude larger than the normal fluid vorticity dipoles [26]. The misalignment of the direction of the relative velocity between the vortex and the normal fluid [indicated by the ruler in Fig. 3 (left)] and the axis of the wake arises from the Iordanskii force (see Methods). In the central and right panels of Fig. 3, we report the PDFs of the streamwise and spanwise normal fluid velocity fluctuations in our single vortex numerical experiment. We observe that the PDFs (center and right panels) mimic the behavior of the corresponding PDFs computed for the turbulent counterflow at the same counterflow velocity $v_{ns}^{(1)} = 0.27$ cm/s reported in Fig. 2 (red curves): skewed and/or with wide exponential tails.

The dipole and the parabolic wake induced by a vortex onto the normal fluid recall the classical Oseen solution of the slow viscous flow past a cylinder of radius a_0 equations [34]. Indeed, the assumptions behind the Oseen solution are well satisfied: the vortex is locally straight (its radius of curvature is $R_c \approx \ell \gg a_0$) hence, the flow is two dimensional, the Reynolds number $\mathrm{Re} = \bar{v}_n^z a_0/\nu_n$ (where ν_n is the kinematic viscosity) is very small: $\mathrm{Re}^{(1)} = 0.3 \times 10^{-5}$ and $\mathrm{Re}^{(2)} = 1 \times 10^{-5}$, and the scales at which we probe the flow are much larger than the cylinder's radius. Focusing on the far field solution at distances larger than the Oseen scale a_0/Re, we recover both the vortex dipole and the parabolic wake in intensity and shape, and the skewed-exponential velocity fluctuation PDFs [33]. The far wake Oseen solution also provides a very good estimate for the velocity fluctuations reported in Fig. 2.

Our results thus suggest that the flow of the normal fluid in a turbulent helium counterflow can be described as the superposition of a uniform background flow generated by the heater and flow disturbances (consisting of small vortex dipoles and large almost parabolic wakes) generated by the vortices via the friction force. The less pronounced tails of the normal fluid velocity fluctuations for $v_{ns}^{(2)} = 0.94$ cm/s (Fig. 2, green curves) arise from the fact that the wake $w^{(2)}$ is larger than the average intervortex spacing $\ell^{(2)} = 94$ μm, hence wakes overlap randomizing the flow. On the contrary, for $v_{ns}^{(1)} = 0.27$ cm/s, $w^{(1)} < \ell^{(1)} = 370$ μm, the wakes tend to be separated, and the velocity statistics of the normal fluid (Fig. 2, red curves) echo the case of an isolated vortex (Fig. 3, central and right panels).

The natural question is whether the normal fluid wakes that we predict can be detected in experiments. Nondestructive visualization of the turbulent normal fluid has been achieved using metastable helium molecules [21], but has not yet probed the length scales considered here. However, measurements obtained via the PTV visualization technique may show the signature of the wakes. Indeed, a recent PTV experiment at large counterflow velocities reported a left-skewed distribution for the streamwise velocity of likely trapped particles (the so-called "slow" particles in Fig. 10 of Ref. [35]), similar to the normal fluid streamwise velocity distributions that we calculate [our Fig. 2 (left)].

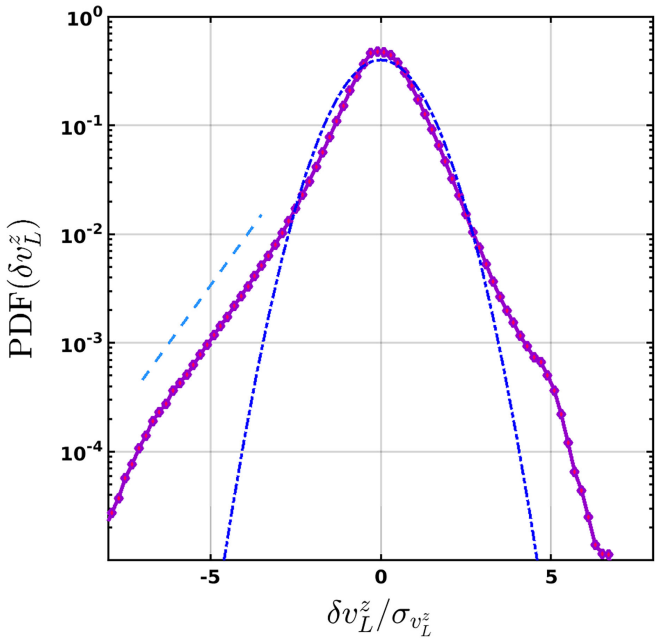

FIG. 4. Vortex statistics. Parameters: $T = 1.5$ K, $v_{ns} = v_{ns}^{(2)} = 0.94$ cm/s. Distribution of streamwise vortex velocity fluctuations PDF(δv_L^z) vs $\delta v_L^z/\sigma_{v_L^z}$ where $\sigma_{v_L^z}$ is the standard deviation of v_L^z. The dot-dashed blue line is the Gaussian fit, and the cyan dashed line is a guide to the eyes to highlight the tail.

A similar left-skewed distribution (see Fig. 4) is recovered when calculating at $v_{ns} = v_{ns}^{(2)}$ (as experiments are performed at large v_{ns}) the distribution of the streamwise vortex velocity fluctuations $\delta v_L^z = v_L^z - \bar{v}_L^z$, where $\mathbf{v}_L$ is the vortex velocity, confirming that the motion of particles trapped on vortices may be indeed approximated with the motion of the vortices themselves [29,36]. It is possible to show [33] that the skewness which characterises δv_n^z [Fig. 2 (left)] contributes to the enhancement of the skewness of δv_L^z (Fig. 4): the experimental signature of the normal fluid wakes is the left-skewed distribution of the streamwise velocity of likely trapped particles in PTV experiments [35].

Finally, it is interesting to notice that the original one-way coupled theory of Schwarz [24] (where $\mathbf{v}_n = \bar{\mathbf{v}}_n$, prescribed *a priori*) predicts that, at $T = 1.5$ K, the vortex tangle drifts, with respect to the superfluid applied flow, at average velocity $\bar{v}_L^z - \bar{v}_s^z \approx 0.35 v_{ns}$ in the direction of v_n^z [31], as a result of the drag exerted by the normal fluid. A subsequent experiment [37] found that the average drift velocity of the vortices is smaller, reporting the upper limit $\bar{v}_L^z - \bar{v}_s^z < 0.2 v_{ns}$ for this temperature, which has been confirmed by more recent numerical and theoretical investigations of the Schwarz model [38,39]. Our two-way coupled simulation finds $\bar{v}_L^z - \bar{v}_s^z \leq 0.15 v_{ns}$, in good agreement with the experiment [37], showing that vortices see a slower normal fluid as a result of the wakes. The issue of the drift of the vortex tangle remains nevertheless open, as it entangles different contributions from anisotropy, two-fluid coupling and wakes.

In conclusion, our numerical experiments predict that counterflow turbulence can be described as the superposition of (i) the superflow and the normal flow (here uniform) which are imposed by the heater, (ii) superfluid velocity fluctuations created by the turbulent vortex lines, and (iii) local perturbations of the normal fluid velocity induced by the friction. Two decades ago theory predicted [22] that the vortex lines are surrounded by small dipolar vorticity structures in the normal fluid. The very small scale of these structures (comparable to the scale of the particles used for PTV visualization) has so far prevented any direct observation. The novel feature revealed by the work presented here is that, alongside the dipolar structures, the vortex lines also induce normal fluid wakes which can be larger than the average intervortex distance and affect the velocity statistics of the normal fluid, as the experiments that we have discussed suggest. One could therefore inquire if such large-scale wakes could also affect thermodynamic quantities [40], leading to interesting new phenomena.

Acknowledgments—We acknowledge discussions with Professor Marco La Mantia, Professor Mathieu Gibert, and Professor Wei Guo. G. K. acknowledges support of Agence Nationale de la Recherche through the project QuantumVIW ANR-23-CE30-0024-02.

Data availability—The data that support the findings of this article are openly available [41].

[1] W. F. Vinen, Proc. R. Soc. A **242**, 493 (1957).
[2] S. Babuin, M. Stammeier, E. Varga, M. Rotter, and L. Skrbek, Phys. Rev. B **86**, 134515 (2012).
[3] E. J. Yarmchuk, M. J. V. Gordon, and R. E. Packard, Phys. Rev. Lett. **43**, 214 (1979).
[4] O. Avenel and E. Varoquaux, Phys. Rev. Lett. **55**, 2704 (1985).
[5] J. T. Mäkinen, S. Autti, P. J. Heikkinnen, J. J. Hosio, R. Hänninen, V. S. L'vov, P. M. Walmsley, V. V. Zavjalov, and V. B. Eltsov, Nat. Phys. **19**, 898 (2023).
[6] C. Peretti, J. Vessaire, É. Durozoy, and M. Gibert, Sci. Adv. **9**, eadh2899 (2023).
[7] E. Fonda, D. Meichle, B. Ouellette, S. Hormoz, and D. Lathrop, Proc. Natl. Acad. Sci. U.S.A. **111**, 4707 (2014).
[8] L. Skrbek, D. Schmoranzer, S. Midlik, and K. R. Sreenivasan, Proc. Natl. Acad. Sci. U.S.A. **118**, e2018406118 (2021).
[9] C. F. Barenghi, H. A. J. Middleton-Spencer, L. Galantucci, and N. G. Parker, AVS Quantum Sci. **5**, 025601 (2023).
[10] H. Hall and W. Vinen, Proc. R. Soc. A **238**, 204 (1956).
[11] H. Hall and W. Vinen, Proc. R. Soc. A **238**, 215 (1956).
[12] T. Zhang and S. W. Van Sciver, Nat. Phys **1**, 36 (2005).
[13] G. P. Bewley, D. P. Lathrop, and K. P. Sreenivasan, Nature (London) **441**, 588 (2006).

[14] M. La Mantia, D. Duda, M. Rotter, and L. Skrbek, J. Fluid Mech., **717**, R9 (2013).
[15] Y. Tang, W. Guo, H. Kobayashi, S. Yui, M. Tsubota, and T. Kanai, Nat. Commun. **14**, 2941 (2023).
[16] W. Kubo and Y. Tsuji, J. Low Temp. Phys. **196**, 170 (2019).
[17] T. Xu and S. V. Van Sciver, Phys. Fluids **19**, 071703 (2007).
[18] L. Galantucci, M. Sciacca, and C. F. Barenghi, Phys. Rev. B **92**, 174530 (2015).
[19] S. Yui, M. Tsubota, and H. Kobayashi, Phys. Rev. Lett. **120**, 155301 (2018).
[20] D. J. Melotte and C. F. Barenghi, Phys. Rev. Lett. **80**, 4181 (1998).
[21] W. Guo, S. B. Cahn, J. A. Nikkel, W. F. Vinen, and D. N. McKinsey, Phys. Rev. Lett. **105**, 045301 (2010).
[22] D. Kivotides, C. F. Barenghi, and D. C. Samuels, Science **290**, 777 (2000).
[23] L. Galantucci, A. Baggaley, C. Barenghi, and G. Krstulovic, Eur. Phys. J. Plus **135**, 547 (2020).
[24] K. W. Schwarz, Phys. Rev. B **38**, 2398 (1988).
[25] D. Kivotides, Phys. Rev. Fluids **3**, 104701 (2018).
[26] L. Galantucci, G. Krstulovic, and C. F. Barenghi, Phys. Rev. Fluids **8**, 014702 (2023).
[27] S. Inui and M. Tsubota, Phys. Rev. B **104**, 214503 (2021).
[28] B. Mastracci, S. Bao, W. Guo, and W. F. Vinen, Phys. Rev. Fluids **4**, 083305 (2019).
[29] B. Mastracci and W. Guo, Phys. Rev. Fluids **3**, 063304 (2018).
[30] N. Mordant, E. Leveque, and J. Pinton, New J. Phys. **6**, 116 (2004).
[31] K. W. Schwarz, Phys. Rev. B **18**, 245 (1978).
[32] C. Barenghi and D. Samuels, J. Low Temp. Phys. **136**, 281 (2004).
[33] See Supplemental Material at http://link.aps.org/supplemental/10.1103/xnyc-321m for methods and details regarding the analytical Oseen solution.
[34] H. Lamb, *Hydrodynamics* (Cambridge University Press, Cambridge, 1932).
[35] P. Švančara, D. Duda, P. Hrubcová, M. Rotter, L. Skrbek, M. La Mantia, E. Durozoy, P. Diribarne, B. Rousset, M. Bourgoin *et al.*, J. Fluid Mech. **911**, A8 (2021).
[36] S. Yui, Y. Tang, W. Guo, H. Kobayashi, and M. Tsubota, Phys. Rev. Lett. **129**, 025301 (2022).
[37] D. D. Awschalom, F. P. Milliken, and K. W. Schwarz, Phys. Rev. Lett. **53**, 1372 (1984).
[38] L. Kondaurova, V. L'vov, A. Pomyalov, and I. Procaccia, Phys. Rev. B **89**, 014502 (2014).
[39] S. K. Nemirovskii, Phys. Rep. **524**, 85 (2013).
[40] S. Nemirovskii, Phys. Fluids **36**, 117156 (2024).
[41] L. Galantucci, G. Krstulovic, C. F. Barenghi (2025), 10.5281/zenodo.17457098.